Atmospheric Pollution Research 6 (2015) 138-146

Atmospheric Pollution Research

www.atmospolres.com

Radiative implication of a haze event over Eastern India

Subin Jose [1], Biswadip Gharai [1], Y. Bhavani Kumar [2], Pamaraju Venkata Narasimha Rao [1]

[1] *Atmospheric and Climate Sciences Group, ECSA, National Remote Sensing Centre (NRSC), Balanagar, Hyderabad–500 037, India*
[2] *National Atmospheric Research Laboratory (NARL), Gadanki–517112, India*

ABSTRACT

Aerosol haze degrades visibility by the process of absorption and scattering of aerosols. In the present study an attempt has been made to characterize the physical and optical properties of aerosols during a haze event on 29 March 2012 and assess its implication on radiative forcing. In this context representative clear (2 March 2012) and normal (19 March 2012) days were identified in terms of their Aerosol Optical Depth (AOD) loading over Hyderabad. On the hazy day, a huge spread of haze was observed over the eastern part of India by MODerate resolution Imaging Spectroradiometer (MODIS) on board Terra satellite which is represented by high Aerosol Optical Depth at 550 nm. In–situ observations on hazy day showed an enhancement of columnar AOD_{500} respectively by 4.5 and 1.8 fold in comparison to clear and normal days. Significant increase in the scattering coefficient and a moderate enhancement of Single Scattering Albedo (SSA) are observed on hazy day compared to normal day. Study also showed that Diffuse–to–Direct– beam irradiance Ratio (DDR) had increased 4.5 times at 496.6 nm spectral band on hazy day. LIDAR (LIght Detection And Ranging) observations on hazy night showed a threefold increase in aerosol backscattering below the Atmospheric Boundary Layer (ABL) compared to normal representative night. The hazy day is characterized by large negative surface forcing (–87.82 W m^{-2}) when compared to normal day (–53.90 W m^{-2}). A large positive enhancement of atmospheric forcing of 30.56 W m^{-2} is observed on hazy day compared to normal day.

Keywords: *Absorption, scattering coefficient, DDR, aerosol backscattering, ARF*

Corresponding Author:
Biswadip Gharai
☎ : *+91-040-23884476*
🖷 : *+91-040-23875932*
✉ : *g.biswadip@gmail.com*

Article History:
Received: 03 April 2014
Revised: 10 August 2014
Accepted: 11 August 2014

doi: 10.5094/APR.2015.016

1. Introduction

Haziness or degree of haze is a measure of light scattering and absorption by aerosols (Husar et al., 1981). Hence it plays a vital role in Earth's radiative balance (Ramanathan et al., 2001) and in visibility degradation (Watson, 2002; Zhang et al., 2010). It is one of the visible effects of air pollution observed most widely by many researchers (Husar et al., 1981). These aerosols can be transported over thousands of kilometers under favorable metrological conditions and reside in the atmosphere for days to weeks (Houghton, 1996), creating a contiguous layer of enhanced concentration of aerosols before being removed from the atmosphere (Fearnside et al., 2005). On regional scale, large spatial extent of haze can create a significant perturbation in Earth's radiative balance as it not only restricts solar radiation to reach the surface but also reduces the rate of long wave emission from the surface (Charlson et al., 1992; Schwartz and Andreae, 1996). A solar radiation deficit of around 7.5% was reported by Ball and Robinson (1982) in some parts of the United States due to haze events.

Since late 1970's natural and anthropogenic atmospheric haze and its spatial and temporal distribution has been creating a lot of interest among the researchers and since then there is a constant effort to understand the physical and chemical properties of haze and its formation mechanisms (Husar et al., 1987). Haze is influenced by its emitting sources, transport, transformation and its removal from the atmosphere (Husar et al., 1981). Sulfate (SO_4^{-2}) has been identified as the dominant species associated with summer haze in Eastern U.S (Wolff, 1984). Tan et al. (2009) have indicated a remarkably rapid increase of secondary pollutants and a significantly higher Organic Carbon (OC)/Elemental Carbon (EC) ratio on a hazy day to a normal day in Guangzhou, China.

Over India, one of the highly populated and fast developing countries, haze/fog is a frequent phenomena under favorable meteorological conditions during the winter but the causes of summer haze are different. Summer haze over these regions is mainly caused by forest fires and agricultural crop residue burning which emits remarkable amounts of carbonaceous and traces gases to the atmosphere (Tripathi et al., 2006; Ramanathan et al., 2007; Badarinath et al., 2009). By these emissions, atmospheric chemistry gets altered and thereby radiative budget of the troposphere. A specific thrust was given during 1999 INDian Ocean EXperiment (INDOEX) campaigns, to understand the role of anthropogenic emissions in formation of Asian haze and its effect on altering radiation budget (Ramanathan et al., 2001). Over Indo Gangetic Plain (IGP), which is characterized as a hot spot of anthropogenic emissions in south Asia (Ramanathan et al., 2007), a nearly 30% increase in EC, OC and Water Soluble Organic Carbon (WSOC) was reported by Ram et al. (2012) during haze and fog events.

Aerosol Radiative Forcing (ARF) can be defined as the variations in the radiative flux at the surface and Top of the Atmosphere (TOA) due to change in aerosol amounts in the atmosphere. ARF depends upon not only aerosols' physical and optical properties but also their horizontal and vertical extent. Based on different kinds of natural or anthropogenic sources of origin, physical and optical properties of aerosols are varying. Aerosols can change their properties during transport as different aerosols often clump together to form complex mixtures. The sign

and magnitude of the aerosol radiative forcing changes based on different aerosol properties (Satheesh and Moorthy, 2005). Sulfate aerosols back scatter the solar radiation and thereby enhance the planetary albedo. In these process sulfate aerosols cools the Earth surface (negative forcing). While in case of absorbing aerosols like Black Carbon (BC), they can change the sign of forcing from negative to positive causing a heating effect (Heintzenberg et al., 1997). When black carbon particles from soot or smoke mix with nitrates and sulfates, or coat the surfaces of dust, they create hybrid particles and thereby alter radiative forcing in a complex way. Because of the inherent problems with satellite observations it is very difficult to characterize the atmospheric aerosols, which enhance the uncertainty in estimating their overall climatic effect (Morgan et al., 2006; Remer and Kaufman, 2006; Yu et al., 2006). Therefore to reduce the uncertainty in estimating ARF, well calibrated in–situ observations are required in conjunction with radiative transfer models and satellite observations.

The main objectives of the present study were to analyze the aerosol properties during a typical hazy day and their implications on radiation using in–situ and satellite based observations. Aerosols' radiative implications during haze event were compared with a clear and a normal day.

2. Site Description

Present study was conducted at the premises of National Remote Sensing Centre (NRSC), Hyderabad (17.47 N, 78.43 E). Hyderabad is the capital of the 5th largest populated state, Andhra Pradesh (84.7 million) in India. Hyderabad alone has a population of 4.01 million (http://censusindia.gov.in/). Vehicular and other anthropogenic emissions are the major sources in the city but episodic long–range transport of dust and emissions from forest fires and agricultural residue burning also influence the city. The four dominant seasons prevailing here are winter (December–February), pre–monsoon (March–May), monsoon (June–September) and post–monsoon (October–November). Fifty years (1951–2000) climatology data of Hyderabad obtained from India Meteorological Department (www.imd.gov.in) shows the maximum and minimum temperatures occur during the months of May and December respectively. The peak maximum temperature of 41.4 °C was recorded during the year 1984 and the lowest value of minimum temperature (10.1 °C) was recorded during 1970. The average annual rainfall of Hyderabad is ~830 mm.

3. Data Sets and Methodology

A number of in–situ along with satellite based measurements were used to study the impact of aerosols on solar radiation during a haze event and are listed in Table 1. Following are the satellite, ground based instruments and radiative transfer model used in the present study.

3.1. Satellite based observations

Terra/Aqua–MODIS. MODerate Resolution Imaging Spectroradiometer (MODIS) (Salomonson et al., 1989; King et al., 1992) is a key instrument onboard TERRA/AQUA satellites having 36 spectral channels. It acquires data in three different spatial resolutions of 250 m (channels 1 and 2), 500 m (channels 3 to 7), and 1 km (channels 8 to 36) covering visible, near infrared, short–wave infrared, and thermal–infrared channels capable of remote sensing clouds, aerosols and water vapor. In the present study, reflective data during a hazy day was obtained from LAADS web site (Level 1 and Atmosphere Archieve and Distribution System). Level 1 MODIS data (HDF EOS), channels 1 (0.645 µm), 3 (0.469 µm) and 4 (0.555 µm) was passed through HDF–EOS Geo Tiff Conversion Tool to reformat and re–project the data. True color composite (Channels 1, 4, 3 combination) of Terra MODIS was used for visual analysis. Level 3 MODIS AOD data at 550 nm obtained from Giovanni site (http://disc.sci.gsfc.nasa.gov/giovanni) was used to analyze the spatial variations of aerosol loading.

3.2. Ground based observations

Sun Photometer. Ground based measurements on aerosols and columnar water vapor content were carried out using Microtops–II sun photometer (Solar instruments, USA) at wavelengths 380 nm, 440 nm, 500 nm, 675 nm, 870 nm and 1 020 nm (Morys et al., 2001). It provides instantaneous AOD by measuring instantaneous solar flux in conjunction with a set of calibration constants and location information from an in–built GPS receiver. Angstrom coefficients (α and β) were calculated using Angstrom relation (Angstrm, 1961; Angstrom, 1961) as:

$$AOD_\lambda = \beta \lambda^{-\alpha} \quad (1)$$

where, AOD_λ is the approximated aerosol optical depth at the wavelength λ, β is the Angstrom's turbidity coefficient, which equals AOD_λ at λ=1 µm, and α is the Angstrom exponent. The Angstrom parameter α is a measure of the ratio of accumulation mode to coarse mode concentrations of the columnar aerosols with higher values representing increased abundance of accumulation mode aerosols (Dumka et al., 2011). The turbidity coefficient β is a measure of the total aerosol loading in the atmosphere (Shaw et al., 1973; Satheesh and Moorthy, 1997). In general uncertainty in microtops measurement are <0.02 for lower wavelength and it is <0.01 for higher wavelengths (Porter et al., 2001; Ichoku et al., 2002) and uncertainties associated with pressure correction for molecular optical depth estimation is ~0.3% at the pressure of 1 013 mb.

Aethalometer. Absorbing black carbon measurements were carried out using AE31 Aethalometer (Magee Scientific, USA). In this instrument, air was passed through a quartz fiber filter tape for a fixed amount of time with a pre–selected flow rate of 3 LPM. Due to deposition of aerosols on fiber tape, light attenuated and this attenuation was measured by Aethalometer at seven wavelengths (370 nm, 470 nm, 520 nm, 590 nm, 660 nm, 880 nm and 950 nm) with 880 nm being the recommended channel for BC measurements. In the present study, spectral absorption coefficient (b_{abs}) was calculated from the attenuation measurements at different wavelengths by adopting the method suggested by Weingartner et al. (2003). Inherent uncertainties in the filter based absorption measurements were discussed elsewhere (Arnott et al., 2005). Uncertainty associated with the Aethalometer measurement is around 10% as reported by the manufacturer.

Nephelometer. Using a well calibrated integrated Nephelometer (TSI 3563, TSI Inc, USA), total and back scattering coefficients of aerosols were measured at three wavelengths (450 nm, 550 nm and 700 nm) during study days. Subsequently aerosol scattering coefficients (σ) were calculated after removing the angular non–idealities following the method suggested by Anderson and Ogren (1998). Details of uncertainties associated with Nephelometer measurements were described by Anderson et al. (1996). They have experimented using nearly monodisperse particles in laboratory and found that predicted and actual Nephelometer (TSI 3563) measurements agreed within experimental uncertainties of ±10%.

Calculated absorption and scattering coefficients were used to derive important aerosol optical properties like extinction coefficient (ε), Single Scattering Albedo (SSA) and asymmetry factor (g). SSA is defined as the ratio of the scattering to the extinction, which can be written as:

$$SSA = \sigma/\varepsilon \quad (2)$$

where, ε is the extinction coefficient defined by the summation of absorption and scattering coefficients.

Table 1. *A set of ground based optical instrumentations and satellite platform used in the present study*

Sl No	Platform	Instrument	Parameter Measured	References
1	Satellite based	MODIS–Terra/Aqua	AOD at 550 nm	King et al. (1992)
2	Ground based	Sunphotometer	Spectral AOD	Morys et al. (2001)
3	Ground based	Pyranometer	Solar Irradiance	www.kippzonen.com/product/13/cmp–11–Pyranmeter
4	Ground based	Aethalometer	Black carbon (μg m^{-3})	Hansen et al. (1984)
5	Ground based	Nephelometer	Scattering coefficient (M m^{-1})	Anderson and Ogren (1998)
6	Ground based	Multi Filter Rotating Shadow band Radiometer	Total and diffuse solar irradiance (W m^{-2})	Harrison et al. (1994); Alexandrov et al. (2002)
7	Ground based	Lidar for Atmospheric Monitoring and Probing (LAMP)	Nocturnal Aerosol Backscattering Coefficient	Kumar (2006)

Asymmetry parameter (g) is the mean value of Cosine of scattering angle over the total solid angle weighted by the phase function (Satheesh et al., 2004). It depends on the size and composition of the particles. Many researchers have provided an alternate approach for deriving asymmetry parameter g using backscattering fraction ($B=\sigma_{bsp}/\sigma_{sp}$),which is the ratio of light scattered into the backward hemisphere (σ_{bsp}) to total light scattering (σ_{sp}) measured by a Nephelometer. We have calculated g by adopting the relation provided by Andrews et al. (2006). The average visibility at 550 nm during the study days was calculated from the following relation (Charlson, 1969):

$$Visibility=[-\ln(0.02)]/\varepsilon \quad (3)$$

Pyranometer. Broad band (285–2 800 nm) measurement of solar irradiance was carried out using a Pyranometer (Model CMP11, Kipp & Zonen, Inc, USA). It measures the ground reaching solar irradiance (W m^{-2}) on a plane surface, which includes both the direct and diffuse solar radiation incident from the hemisphere above. Diurnal variation of solar irradiance was analyzed to characterize the haze event in comparison to that of a clear day observations. As per manufacturer of CMP11, directional (up to 80° with 1 000 W m^{-2} beam) and tilt errors are respectively <10 W m^{-2} and <0.2%.

MFRSR. The Multi–Filter Rotating Shadow band Radiometer (MFRSR) uses narrow bands at 415.6 nm, 495.7 nm, 614.6 nm, 672.8 nm, 868.7 nm and 936.6 nm with FWHM ~10 nm to measure direct normal, total horizontal, and diffuse horizontal irradiance (Harrison et al., 1994). In the present study, spectral irradiance data obtained from MFRSR was analyzed to investigate the Diffuse–to–Direct beam irradiance Ratio (DDR) to characterize the haze event. The DDR minimizes any instrumental error in diffuse and direct beam irradiance (Meloni et al., 2007) and it is reasonably accurate (Halthore et al., 2004). Since DDR is a function of Solar Zenith Angle (SZA), a single SZA (=40°) was chosen for the current analysis. The primary uncertainty introduced by the MFRSR measurements is that of the extraterrestrial response inferred from Langley regression. Harrison et al. (1994) have discussed in detail the accuracy of this procedure; the standard deviation of this inferred response from single retrievals at a difficult site is approximately 5%.

LAMP. LAMP stands for LIDAR for Atmospheric Measurement and Probing. It is an industrial lidar system developed under the license from National Atmospheric Research Laboratory (NARL), a Department of Space unit, located at Gadanki in the southern part of India. The LAMP system is fabricated at General Optics (Asia) ltd., Pondicherry under the supervision of NARL. The LAMP is a high performance compact lidar system that operates on the principle of micro pulsing. The LAMP system contains a diode–pumped Nd–YAG laser, a co–axial transceiver for transmitting the laser pulses and detecting the collected photons, a dedicated data acquisition system, and a computer control and interface system. It uses low pulse energy laser energy operates at 532 nm wavelength for profiling the atmosphere. The technical configuration of LAMP system is described elsewhere (Kumar, 2006). Laser light at 532 nm interacts with particles and molecules in the atmosphere, by which define the amount of backscattering. The altitude profile of molecular number density was calculated using the equation suggested by Reddy and Kumar (2013), employing the vertical profiles of temperature and pressure data obtained from NOAA READY site (http://www.ready.noaa.gov/). Backscattering coefficient from the lidar signal was then calculated using the inversion technique suggested by Klett (1981). The lidar signals are background and range corrected before subjecting to inversion analysis. Altitude profiles of aerosol backscattering coefficient were computed by subtracting the altitude dependent molecular backscattering from the total backscattering.

3.3. SBDART

Santa Barbara DISORT Atmospheric Radiative Transfer (SBDART) is a software tool that computes plane–parallel radiative transfer in clear and cloudy conditions within the earth's atmosphere and at the surface. The code is well suited for a wide variety of atmospheric radiative energy balance and remote sensing studies (Ricchiazzi et al., 1998). SBDART uses numerically stable algorithm to solve the equations of plane–parallel radiative transfer in vertically inhomogeneous atmosphere. The measured and derived physical and optical parameters like AOD, *SSA*, g, α and visibility were used to estimate the aerosol radiative forcing in ShortWave (SW) region (0.25 μm to 4 μm) by incorporating into SBDART model. Since the study site Hyderabad, is an urban area, surface albedo was taken as a combination of two basic surface types, i.e. sand and vegetation. In our study, we considered tropical atmospheric profile to run SBDART separately with and without aerosols to estimate aerosol radiative forcing at the Top of the Atmosphere (TOA) and surface. The difference between the TOA and surface forcing was taken as atmospheric forcing, which represented the amount of energy trapped within the atmosphere due to the presence of aerosols. The overall uncertainty in the estimated forcing, is due to the small deviations in the simulations and uncertainties in the surface parameters used as input to SBDART. It has been reported by Ricchiazzi et al. (1998) that the accuracy of SBDART is within 3% when compared with precise ground observations in SW range.

4. Results and Discussion

4.1. Haze event

Synoptic view of satellite observations on a hazy day (29 March 2012) as observed by MODIS Terra is shown in Figure 1a. True color composition of satellite data observations on hazy day showed a huge spread of haze over the eastern part of

the Indian region. The visual appearance of haze was investigated using Terra MODIS derived AOD_{550} data, which were assigned to four different colors corresponding to four regrouped categories: <0.35, 0.35–0.55, 0.55–0.75 and >0.75 values as shown in Figure 1b. Detailed procedure is given elsewhere (Gharai et al., 2013). From the Figure 1, it is evident that hazy appearance over the entire eastern part of India is represented by high AOD values (>0.55). This high value of AOD virtually reduces the visibility and thereby degrades the image contrast over eastern India as appeared in Figure 1a.

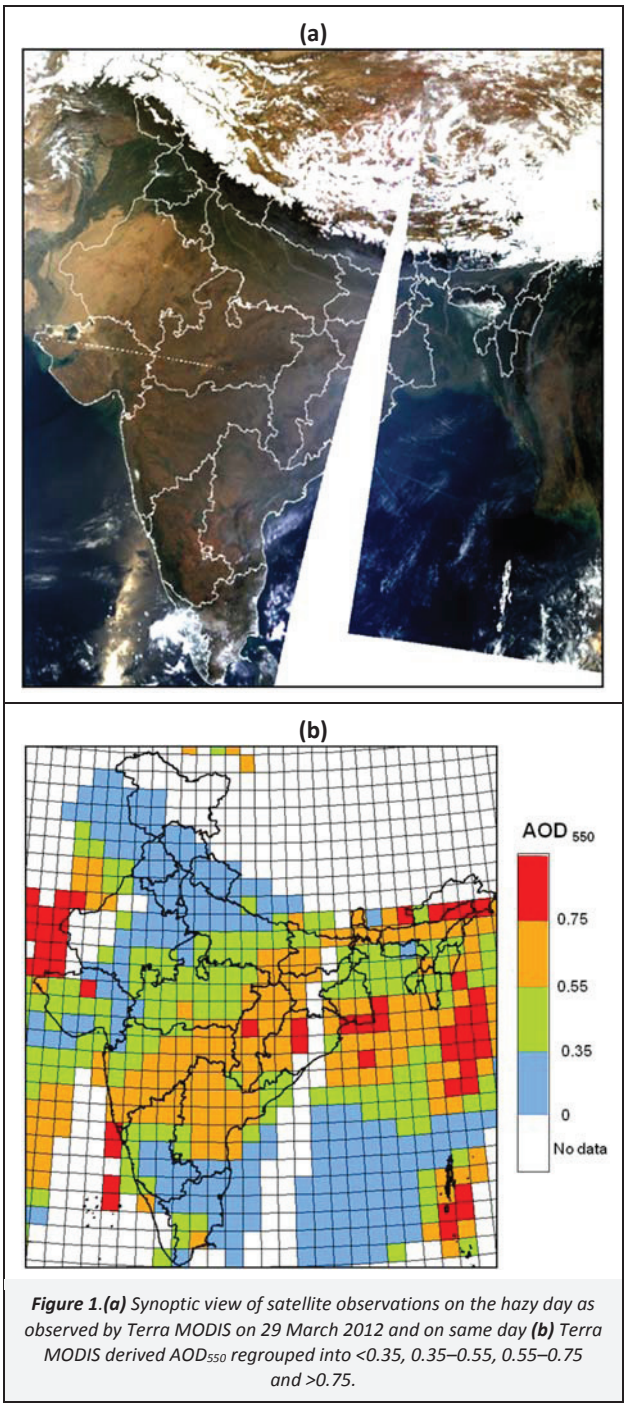

Figure 1.(a) *Synoptic view of satellite observations on the hazy day as observed by Terra MODIS on 29 March 2012 and on same day* ***(b)*** *Terra MODIS derived AOD_{550} regrouped into <0.35, 0.35–0.55, 0.55–0.75 and >0.75.*

To investigate the general level of AOD over Hyderabad during pre–monsoon (March, April and May), we have analyzed four years (2009–2012) in–situ AOD observations carried out over Hyderabad using hand held Sun–photometer. Frequency distribution of daily averaged AOD_{500} and Angstrom exponent (α) calculated (440 nm–870 nm) using Equation (1) over a period of 2009–2012 are, respectively, shown in Figure 2a and Figure 2b**.** The bin intervals for AODs and "α" were set up to 0.20. It can be seen from the figure that during pre–monsoon, more than 72% of the AODs are between 0.5–0.9 and only 0.73% of the AODs are below 0.3. The AODs with values greater than one occurred about 15% of time of the total data sets analyzed. Therefore, a daily averaged AOD_{500} of 0.26 and 0.62 observed on 2 and 19 March 2012 respectively are considered to be clear and normal days in the current study. In addition these, two dates are close to the haze event and hence considered as reference study days. The frequency histogram of "α" in the years 2009–2012 during pre–monsoon (Figure 2b) clearly indicates the presence of a mixture of fine and coarse mode particles. The range of α varies mainly from 0.4 to 1.4 accounting for 93.9% of the total occurrence, with a peak between 1.1 and 1.2.

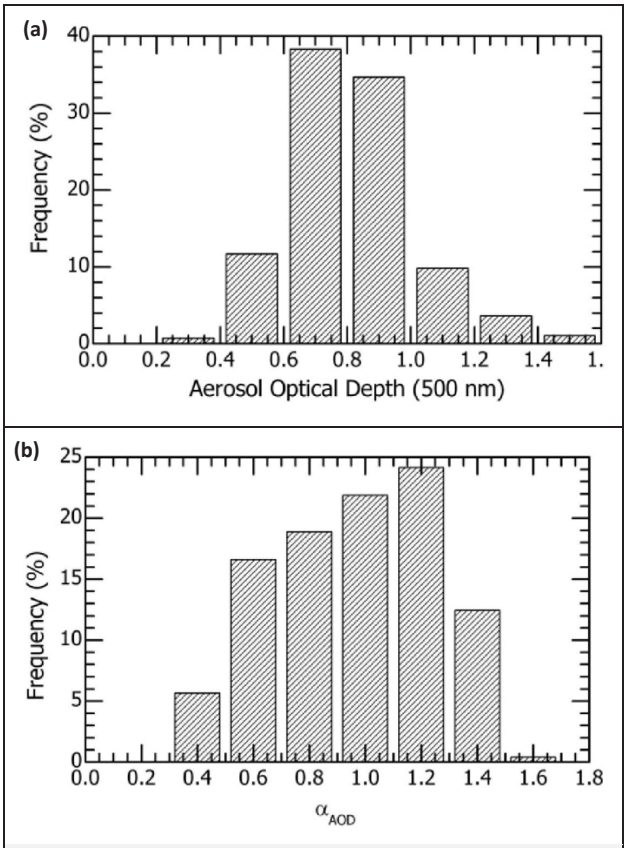

Figure 2. (a) *Frequency distributions of daily averaged AOD_{500} and* ***(b)*** *Angstrom exponent (α) (440 nm–870 nm) during 2009–2012.*

4.2. Spectral characteristics of aerosol optical properties

The spectral variation of daily averaged AOD during the study days based on in–situ observations is shown in Figure 3a. Study revealed that on a hazy day, the columnar AOD_{500} had enhanced respectively by 4.5 and 1.8 fold in comparison to clear and normal days. Angstrom coefficient α showed a very high value of 1.15 on hazy day compared to clear day (α=0.33), which implies the enhancement of accumulation mode of aerosols in lower troposphere on 29 March 2012.

Daily averaged absorption coefficient (b_{abs}) calculated using data from Aethalometer is shown in Figure 3b. No significant variations of mean absorption coefficient at 880 nm were observed during the haze event compared to that of clear and normal days.

The spectrally dependent aerosol absorption coefficient is given by a power law relationship:

$$b_{abs}(\lambda) = C\,\lambda^{-AAE} \quad (4)$$

where, b_{abs} (λ) is the aerosol absorption coefficient, *C* is a constant, and AAE is Absorption Angstrom Exponent. The AAE for absorption coefficient is calculated by negative slope of absorption vs. wavelength in a log–log plot (for wavelengths 370 nm to 950 nm). Thus the value of AAE is a measure of the strength of the spectral variation in aerosol light absorption. AAE ~2.5 indicates strong spectral dependence on biomass burning aerosols and AAE ~1 indicates weak spectral dependence on the motor vehicle aerosols (Kirchstetter et al., 2004; Bergstrom et al., 2007; Praveen et al., 2011). An AAE value between 1 and 2 could be an indication of aerosols of mixed origin of fossil as well as biomass fuels (Praveen et al., 2011). An AAE=1.2 was reported during SAFARI, 2000 for haze samples aloft (Bergstrom et al., 2004). In our study, mean AAE values calculated were 0.98, 1.03 respectively for representative clear and normal days. Whereas on haze day it was 1.10 (1<AAE <2), which indicates the presence of mixed origin of fossil and biomass fuels on that day. To investigate the effect of forest/ agricultural residue burning on the haze event, we analyzed the spatial distribution of MODIS fire locations (during 09:00–10:30 LT) in conjunction with the spread of hazy appearance on MODIS true color composite (not presented here). It was observed that a moderate number of fire locations coincide with the spread of haze layer, indicated its partly contribution on haze formation. Moreover, since the study period is in peak summer and Hyderabad being an urban site, background local dust is one of the components, which mix up with other aerosols originated from different sources during this period.

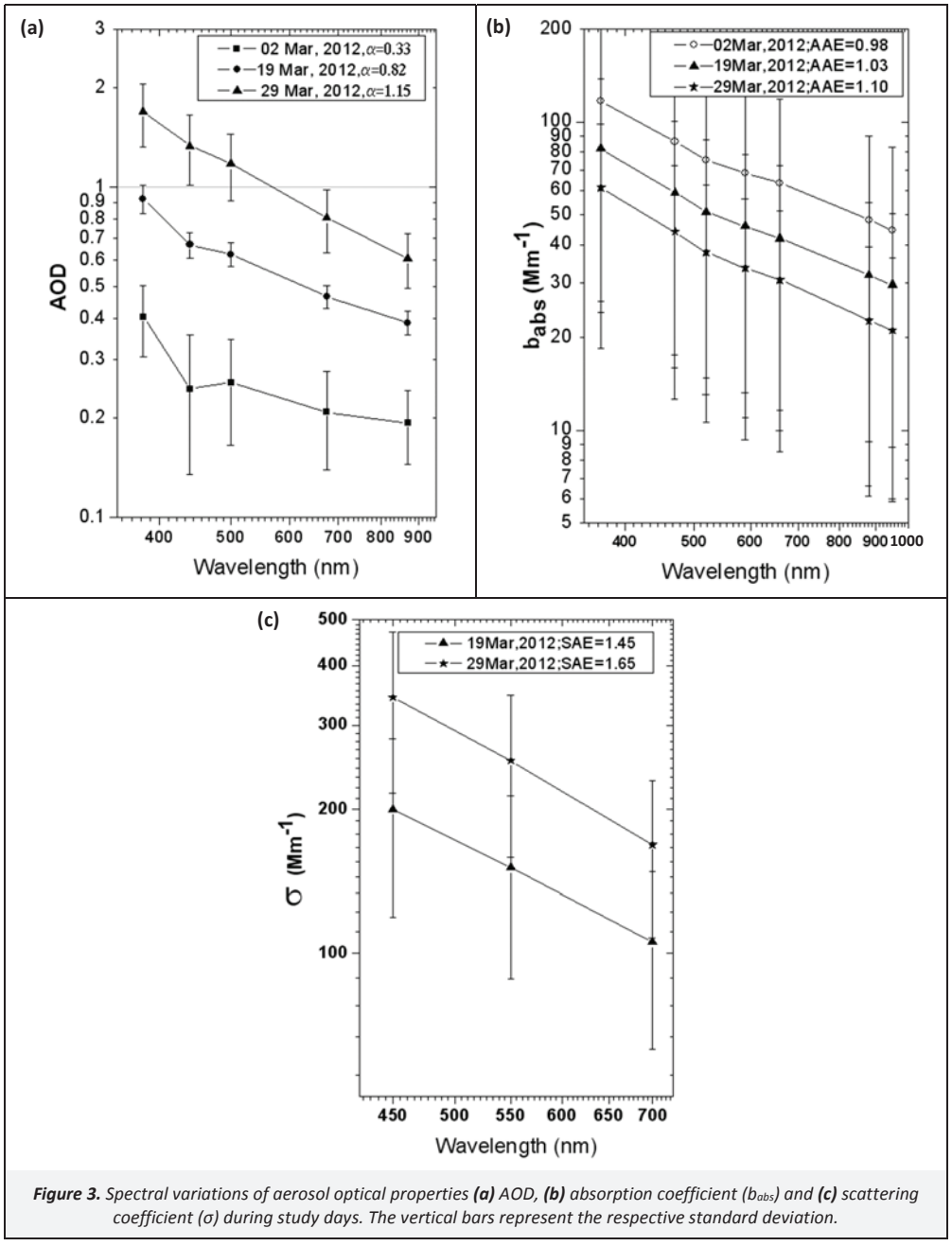

Figure 3. *Spectral variations of aerosol optical properties* ***(a)*** *AOD,* ***(b)*** *absorption coefficient (b_{abs}) and* ***(c)*** *scattering coefficient (σ) during study days. The vertical bars represent the respective standard deviation.*

Spectral variation of day averaged scattering coefficient is illustrated in Figure 3c. Aerosol scattering coefficient (σ) has increased from 150 Mm^{-1} to 250 Mm^{-1} at 550 nm during haze event compared to that of a normal day. Nephelometer observations were not available on 2 March 2012 as it was under calibration process. The spectral dependence of aerosol scattering coefficient follows same Angstrom power law as described by Equation (4). The Scattering Angstrom Exponent (SAE) was calculated by negative slope of scattering vs. wavelength in a log–log plot (for wavelengths 450 nm to 700 nm). Dubovik et al. (2002) have suggested that the scattering Angstrom exponent value around 2 implies an aerosol volume size distribution with scattering dominated by small particles (diameter <1 µm), while a volume distribution dominated by coarse particles (diameter >1 µm) has typically a smaller value around 1. In our study site SAE has increased to 1.65 on haze day compared to normal day (SAE=1.45) attributed to the enhancement of fine mode scattering particles. To examine the possibility of enhancement of AOD on the haze day due to presence of high water vapor content, we analyzed the columnar water vapor data using microtops sun–photometer measurement. Study shows that during this period average columnar water vapor has a little enhancement from 1.2–1.3 g cm^{-1}, which suggest that the contribution of water vapor on altering scattering/absorbing properties is not very significant. Study revealed that haze formation on 29 March 2012 was due to a combination of different phenomenons like fossil fuel and biomass burning, local and long–range transport of dust and smoke.

The SSA values calculated using Equation (2) at 550 nm using in–situ observations on the normal and the hazy days were 0.84 and 0.87, respectively indicating the enhancement of scattering particles on the haze day. A similar SSA value of 0.88 at 550 nm during hazy sky days was reported by Niranjan et al. (2007). In the present study, average asymmetry parameter g on hazy day was found to be 0.55. The value of *g* ranges between –1 for entirely backscattered light to +1 for entirely forward scattered light (Lemaitre et al., 2010). In our study on the hazy day *g* value increased to 0.55 from 0.52 as observed on the normal day, which could be attributed by enhancement of forward scattering due to presence of large number of particles on the haze day. The visibility calculated using Equation (3) for the hazy day showed a reduction of about 30% from the normal day.

4.3. Haze impact on solar radiation

Diurnal variations of solar irradiance on study days observed by Pyranometer (CMP11) in SW region (285–2 800 nm) showed a clear reduction of down welling solar radiation due to the enhanced aerosol layer on the hazy day (figure not shown). Study revealed that average solar irradiance reduced by 26% on the hazy day (morning 06:30 h to evening 18:30 h) when compared to a clear day.

To access the impact of AOD on spectral solar radiation, observed AOD and diffuse to direct ratio (DDR) at different MFRSR spectral wavelengths were analyzed. The scatter plot of AOD and DDR is shown in Figure 4. It is clear from the figure that the value of DDR during the clear day is much lower than that on the hazy day. The increase in aerosol loading and spreading over a large area (Figure 1) resulted in higher DDR of solar irradiance on hazy day as evident in this figure. In the Figure 4, DDR values are plotted for the same solar zenith angle (40°) for clear, normal, and hazy days for comparison. Study revealed that abundance of fine mode particles has modified the DDR at different spectral wavelengths. It is also seen from the figure that DDR differences during hazy day in comparison to other study days are more pronounced in shorter wavelengths than that of longer wavelengths. This indicates the large presence of scattering particles on the hazy day. Study also showed that DDR actually increased by 4.5 times at 496.6 nm from clear day to hazy day.

4.4. LAMP observations

Using the LAMP, nocturnal loading of aerosols were analyzed for the study period. LAMP was operated in the evening hours (after sunset) on cloudless nights. In the Figure 5 top panel shows the time height cross section of range corrected backscattered photons collected between 19:00–06:00 LT (Local Time) on the observational nights at the lidar site. Bottom panel shows the backscattering of nocturnal aerosol and their altitudinal variations during 22:00–22:30 LT, which was chosen as a representative window during the three study nights. The vertical profiles of the backscatter coefficient are averaged for 30 minutes (22:00–22:30 LT). A large vertical variation of aerosols was observed during the study nights. The variation of the aerosol vertical profiles in three study days could be related to many meteorological and physical parameters like convection, dynamics of ABL, long–range transport of aerosols and its associated properties and horizontal and vertical motion of the wind. A deep pronounced aerosol rich layer below the atmospheric boundary layer (ABL<2.5 km) was observed on the hazy night. A threefold enhancement of aerosol backscattering was observed below the ABL height on 29 March 2012 during 22:00–22:30 LT compared to normal representative night of 19 March 2012. It was also observed that the aerosol layer has pushed the ABL to a higher altitude on the hazy night as evident in the top panel of Figure 5. Presence of large scattering aerosols during day time is confined mostly below the ABL during night time of haze event. Cloud formation is also observed on hazy night after 23:00 LT above the ABL, which is evident by the high backscattered photon counts as shown in the top panel of Figure 5. This can be explained by the mixing of elements between the ABL and the haze layer.

4.5. Aerosol radiative forcing

The possible reduction of solar irradiance due to presence of large spread of scattering aerosols on a hazy day was investigated using the radiative transfer model SBDART (Ricchiazzi et al., 1998). The averaged diurnal aerosol radiative forcing at TOA and surface are estimated using measured aerosol properties and derived parameters as inputs to SBDART. The amount of energy trapped within the atmosphere due to presence of aerosols is the difference between TOA and surface forcing. Aerosol radiative forcing was estimated independently for the haze day and the normal day as shown in Figure 6. Negative forcing was observed both at TOA and at the surface for both the study days. During the normal day, surface and TOA aerosol forcing estimated are respectively –53.90 W m^{-2} and –6.24 W m^{-2}. On the haze day (29 March 2012) a significantly increased negative surface forcing of –87.82 W m^{-2} was observed. This was due to the presence of large scattering particles on hazy day inhibiting the solar radiation reaching the surface. Magnitude of change in surface forcing (diurnally averaged) in SW region calculated using SBDART (33.92 W m^{-2}) is in agreement with the Pyranometer observation (31.81 W m^{-2}) when the hazy day is compared with the normal day.

The energy trapped within the atmosphere during normal and hazy days are 47.66 W m^{-2} and 78.22 W m^{-2}, respectively. The enhancement of atmospheric positive forcing can be attributed to the confinement of aerosols at the lower atmosphere during hazy sky which is also supported by the nocturnal observation by LAMP. We tried to explore the consequence of haziness on prevailing air temperature. Meteorological data available (www.mosdac.gov.in) near Hyderabad (78.59 E, 17.34 N) was analyzed on the hazy day and compared with immediately two days before the haze incident occurred. Study revealed that there was an enhancement of daytime average air temperature ~1.5 °C on the hazy day when

compared with the average temperatures of previous two days (27–28 March 2012) whereas nighttime difference observed was >2 °C. This happened because the outgoing long wave radiation from the Earth's surface was trapped by the excess aerosols prevailed on the hazy day and thereby increased the air temperature. Since a deep pronounced aerosol rich layer was observed at lower heights of the atmosphere on the hazy night, the air temperature increased in a relatively higher rate than that compared with day time.

We calculated the maximum possible effect on radiative forcing during the normal and hazy days independently after considering the maximum uncertainty involved in inputting to SBDART. Study revealed that maximum uncertainty in radiative forcing calculation at surface would vary about 2.13 W m^{-2} and 5.93 W m^{-2} respectively on normal and hazy days. Similarly in case of atmosphere, it could deviate by maximum of 4.62 W m^{-2} and 9.2 W m^{-2} on normal and hazy days, respectively.

5. Conclusions

In this study we investigated the aerosol optical properties and their radiative implications over eastern India during a haze event and compared with normal day observations using in–situ and satellite data. The results of the study show:

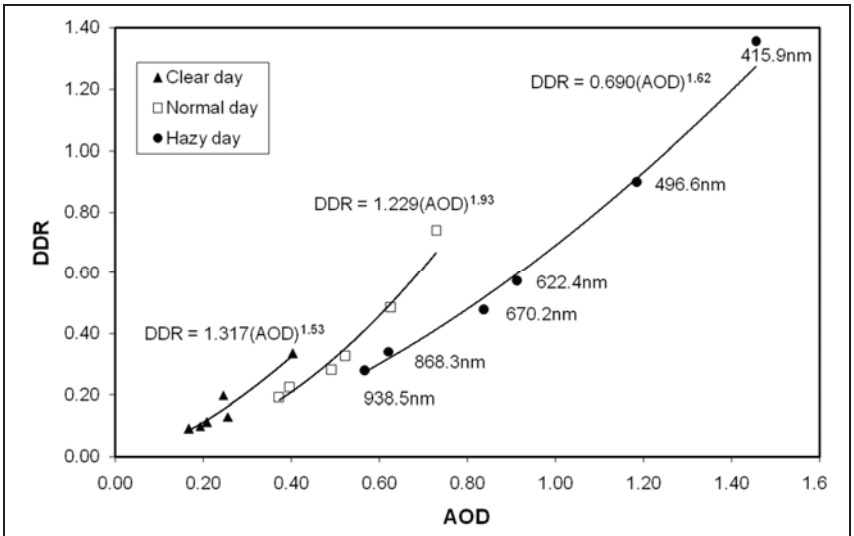

Figure 4. *Variation of Diffuse to Direct Ratio (DDR) with AOD at different wavelengths on study days.*

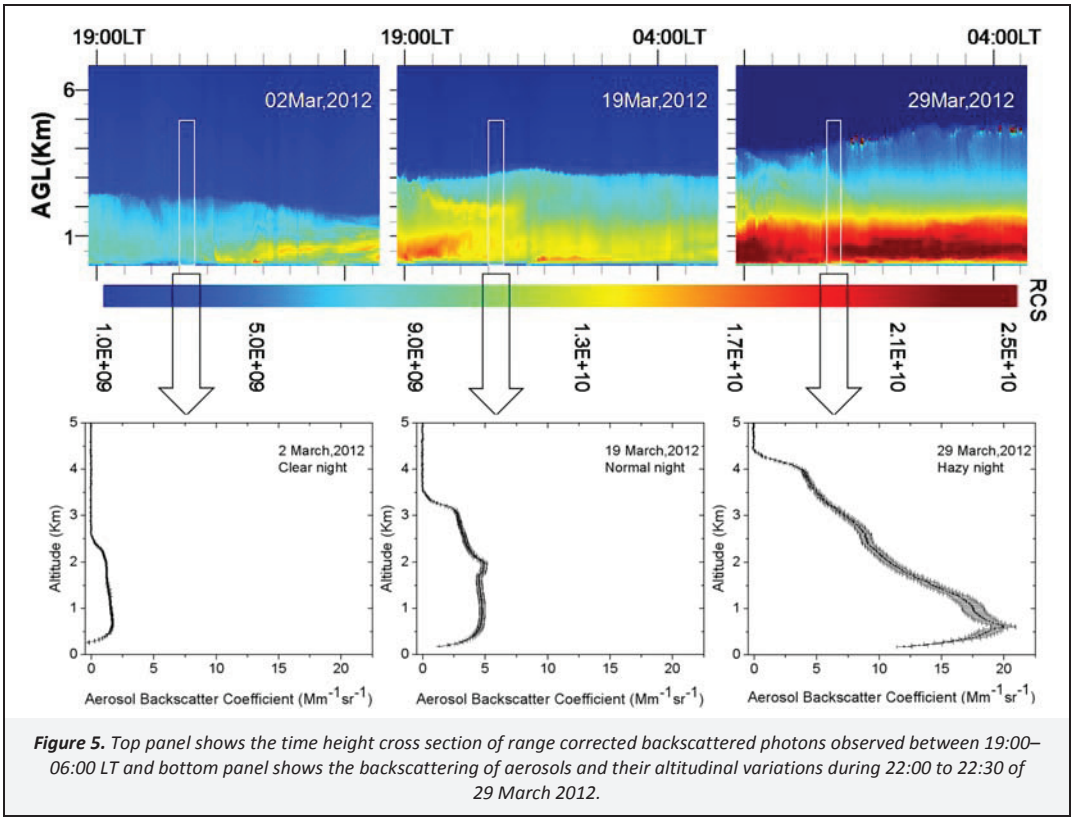

Figure 5. *Top panel shows the time height cross section of range corrected backscattered photons observed between 19:00–06:00 LT and bottom panel shows the backscattering of aerosols and their altitudinal variations during 22:00 to 22:30 of 29 March 2012.*

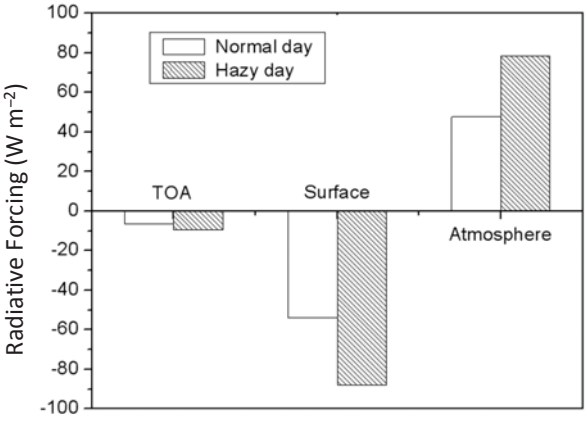

***Figure 6**. SBDART model derived aerosol radiative forcing estimates on 19 March 2012 (normal day) and 29 March 2012 (Hazy day).*

- Huge spread of haze over the eastern Indian region was observed by MODIS onboard Terra satellite on 29 March 2012 at LT 10:30 and was represented by high AOD_{550} (>0.55). This could be due to a combination of fossil fuel and biomass burning, local and long–range transport of dust and smoke.
- On the hazy day, columnar AOD_{500} enhanced respectively by 4.5 and 1.8 fold in comparison to clear and normal days; likewise, the Angstrom coefficient also showed a sharp increase suggesting the abundance of fine mode particles.
- Solar irradiance reduced by 26% on the hazy day in comparison to clear days.
- Significant increase in scattering coefficient was observed on the hazy day, which in turn increased the value of SSA from 0.84 to 0.87 in comparison to a normal day.
- At the same solar zenith angle (40°), DDR had actually increased 4.5 times at 496.6 nm spectral band indicating the presence of large number of scattering particles on the hazy day compared with the clear day.
- A threefold enhancement of aerosol backscattering has been observed below the ABL height on hazy night during 22:00–22:30 LT compared to normal representative night of, 19 March, 2012.
- About 30% reduction of visibility was estimated on the hazy day compared to normal day of 19 March, 2012.
- The hazy day is characterized by large negative surface forcing value (~ –87.82 W m^{-2}) in comparison to a normal day (~ –53.90 W m^{-2}) as enhanced aerosols on hazy day obstruct the incoming solar irradiance. A large positive enhancement of atmospheric forcing (30.56 W m^{-2}) was observed on the hazy day. Maximum uncertainties in radiative forcing calculation at surface (atmosphere) vary between 2.13 W m^{-2} (4.62 W m^{-2}) and 5.93 W m^{-2} (9.2 W m^{-2}) on normal and hazy days respectively.

Acknowledgments

The authors thank Director, NRSC for his encouragement of this work. This activity has been supported by Aerosol Radiative Forcing over India (ARFI) project under ISRO–GBP. We acknowledge MODIS fire team for acquiring the MODIS active fire location. We would like to thank the MODIS Science Data Support Team for processing MODIS aerosol data and gratefully acknowledge the NOAA Air Resources Laboratory (ARL) for providing the vertical profiles of temperature and pressure data used in this study. The authors are grateful to Dr. Vijay Kumar Nair for his valuable suggestions during this work. Authors would like to thanks all the reviewers and the Chief editor for their valuable comments for improving the manuscript in the present form.

References

Alexandrov, M.D., Lacis, A.A., Carlson, B.E., Cairns, B., 2002. Remote sensing of atmospheric aerosols and trace gases by means of Multifilter Rotating Shadowband Radiometer. Part I: Retrieval algorithm. *Journal of the Atmospheric Sciences*, 59, 524-543.

Angstrom, A., 1964. The parameters of atmospheric turbidity. *Tellus* 16, 64–75.

Angstrom, A., 1961. Techniques of determining the turbidity of the Atmosphere. *Tellus* 13, 214–223.

Anderson, T.L., Ogren, J.A., 1998. Determining aerosol radiative properties using the TSI 3563 integrating nephelometer. *Aerosol Science and Technology* 29, 57–69.

Anderson,T.L., Covert, D.S., Marshall, S.F., Laucks, M.L., Charlson, R.J., Waggoner, A.P., Ogren, J.A., Caldow, R.,Holm, R.L.,Quant, F.R., Sem, G.J., Wiedensohier, A., Ahiquist, N.A., Bates, T.S.,1996. Performance characteristic of a high–sensitivity, three–wavelength, total scatter/backscatter nephelometer. *Journal of Atmospheric and Oceanic Technology*, 13,967–986.

Andrews, E., Sheridan, P.J., Fiebig, M., McComiskey, A., Ogren, J.A., Arnott, P., Covert, D., Elleman, R., Gasparini, R., Collins, D., Jonsson, H., Schmid, B., Wang, J., 2006. Comparison of methods for deriving aerosol asymmetry parameter. *Journal of Geophysical Research–Atmospheres* 111, art. no. D05S04.

Arnott, W.P., Hamasha, K., Moosmuller, H., Sheridan, P.J., Ogren, J.A., 2005. Towards aerosol light–absorption measurements with a 7–wavelength aethalometer: Evaluation with a photoacoustic instrument and 3–wavelength nephelometer. *Aerosol Science and Technology* 39, 17–29.

Badarinath, K.V.S., Kharol, S.K., Sharma, A.R., 2009. Long–range transport of aerosols from agriculture crop residue burning in Indo–Gangetic plains–a study using lidar, ground measurements and satellite data. *Journal of Atmospheric and Solar–Terrestrial Physics* 71, 112–120.

Ball, R.J., Robinson, G.D., 1982. The origin of haze in the central united–states and its effect on solar irradiation. *Journal of Applied Meteorology* 21, 171–188.

Bergstrom, R.W., Pilewskie, P., Russell, P.B., Redemann, J., Bond, T.C., Quinn, P.K., Sierau, B., 2007. Spectral absorption properties of atmospheric aerosols. *Atmospheric Chemistry and Physics* 7, 5937–5943.

Bergstrom, R.W., Pilewskie, P., Pommier, J., Rabbette, M., Russell, P.B., Schmid, B., Redemann, J., Higurashi, A., Nakajima, T., Quinn, P.K., 2004. Spectral absorption of solar radiation by aerosols during ACE–Asia. *Journal of Geophysical Research–Atmospheres 109*, art. no. D19S15.

Charlson, R.J., Schwartz, S.E., Hales, J.M., Cess, R.D., Coakley, J.A., Hansen, J.E., Hofmann, D.J., 1992. Climate forcing by anthropogenic aerosols. *Science* 255, 423–430.

Charlson, R. J., 1969. Atmospheric visibility related to aerosol mass concentration: review. *Environmental Science & Technology*, 3, 913–918.

Dubovik, O., Holben, B.N., Lapyonok, T., Sinyuk, A., Mishchenko, M.I., Yang, P., Slutsker, I., 2002. Non–spherical aerosol retrieval method employing light scattering by spheroids. *Geophysical Research Letters* 29, art. no. 1415.

Dumka, U.C., Moorthy, K.K., Tripathi, S.N., Hegde, P., Sagar, R., 2011. Altitude variation of aerosol properties over the Himalayan range inferred from spatial measurements. *Journal of Atmospheric and Solar–Terrestrial Physics* 73, 1747–1761.

Fearnside, P.M., Laurance, W.F., Albernaz, A.K.M., Vasconcelos, H.L., Ferreira, L.V., 2005. A delicate balance in Amazonia–response. *Science Washington* 307, 1045–1045.

Gharai, B., Jose, S., Mahalakshmi, D.V., 2013. Monitoring intense dust storms over the Indian region using satellite data–a case study. *International Journal of Remote Sensing* 34, 7038–7048.

Halthore, R.N., Miller, M.A., Ogren, J.A., Sheridan, P.J., Slater, D.W., Stoffel, T., 2004. Further developments in closure experiments for surface diffuse irradiance under cloud–free skies at a continental site. *Geophysical Research Letters* 31, art. no. L07111.

Hansen, A.D.A., Rosen, H., Novakov, T., 1984. The aethalometer—an instrument for the real-time measurement of optical absorption by aerosol particles. *Science of the Total Environment* 36, 191-196.

Harrison, L., Michalsky, J., Berndt, J., 1994. Automated multifilter rotating shadow–band radiometer–an instrument for optical depth and radiation measurements. *Applied Optics* 33, 5118–5125.

Heintzenberg, J., Charlson, R. J., Clarke, A. D., Liousse, C., Ramaswamy, V., Shine, K. P., Helas, G., 1997. Measurements and modeling of aerosol single–scattering albedo: Progress, problems and prospects. *Beitraege zur Physik der Atmosphaere* 70, 249–263

Houghton, J.T., 1996. Climate Change 199. The Science of Climate Change*:* Contribution of Working Group I to the Second Assessment Report of the Intergovernmental Panel on Climate Change, Cambridge University Press.

Husar, R. B., Patterson, D. E., Wilson, W. E., 1987. Haze Climate of the United States. U.S. Environmental Protection Agency, Atmospheric Sciences Research Laboratory, Report Number EPA/600/S 3–86/071.

Husar, R.B., Holloway, J.M., Patterson, D.E., Wilson, W.E., 1981. Spatial and temporal pattern of eastern–United–States haziness–a summary. *Atmospheric Environment* 15, 1919–1928.

Ichoku, C., Levy, R., Kaufman, Y.J., Remer, L.A., Li, R.R., Martins, V.J., Holben, B.N., Abuhassan, N., Slutsker, I., Eck, T.F., Pietras, C., 2002. Analysis of the performance characteristics of the five–channel microtops II sun photometer for measuring aerosol optical thickness and precipitable water vapor. *Journal of Geophysical Research–Atmospheres* 107, art. no. 4714.

King, M.D., Kaufman, Y.J., Menzel, W.P., Tanre, D., 1992. Remote–sensing of cloud, aerosol, and water–vapor properties from the moderate resolution imaging spectrometer (MODIS). *LEEE Transactions on Geoscience and Remote Sensing* 30, 2–27.

Kirchstetter, T.W., Novakov, T., Hobbs, P.V., 2004. Evidence that the spectral dependence of light absorption by aerosols is affected by organic carbon. *Journal of Geophysical Research*–Atmospheres 109, art. no. D21208.

Klett, J.D., 1981. Stable analytical inversion solution for processing lidar returns. *Applied Optics* 20, 211–220.

Kumar, Y.B., 2006. Portable lidar system for atmospheric boundary layer measurements. *Optical Engineering* 45, art. no. 076201.

Lemaitre, C., Flamant,C. , Cuesta,J., Raut, J.C., Chazette, P., Formenti, P. Pelon, J., 2010. Radiative forcing associated with a springtime case of Bodele and Sudan dust transport over West Africa. *Atmospheric Chemistry and Physics Discuss*ion 10, 8811–8859.

Meloni, D., di Sarra, A., Biavati, G., DeLuisi, J.J., Monteleone, F., Pace, G., Piacentino, S., Sferlazzo, D.M., 2007. Seasonal behavior of Saharan dust events at the Mediterranean island of Lampedusa in the period 1999–2005. *Atmospheric Environment* 41, 3041–3056.

Morgan, M.G., Adams, P.J., Keith, D.W., 2006. Elicitation of expert judgments of aerosol forcing. *Climatic Change* 75, 195–214.

Morys, M., Mims, F.M., Hagerup, S., Anderson, S.E., Baker, A., Kia, J., Walkup, T., 2001. Design, calibration, and performance of microtops II handheld ozone monitor and sun photometer. *Journal of Geophysical Research–Atmospheres* 106, 14573–14582.

Niranjan, K., Sreekanth, V., Madhavan, B.L., Moorthy, K.K., 2007. Aerosol physical properties and radiative forcing at the outflow region from the indo–gangetic plains during typical clear and hazy periods of wintertime. *Geophysical Research Letters* 34, art. no. L19805.

Porter, J.N., Miller, M., Pietras, C., Motell, C., 2001. Ship–based sun photometer measurements using microtops sun photometers. *Journal of Atmospheric and Oceanic Technology* 18, 765–774.

Praveen, P. S., Ahmed, T., Kar, A., Rehman, I. H., Ramanathan, V., 2011. Link between local scale BC emissions and large scale atmospheric solar absorption. *Atmospheric Chemistry and Physics Discussions*, 11, 21319–21361.

Ram, K., Sarin, M.M., Sudheer, A.K., Rengarajan, R., 2012. Carbonaceous and secondary inorganic aerosols during wintertime fog and haze over urban sites in the indo–gangetic plain. *Aerosol and Air Quality Research* 12, 359–370.

Ramanathan, V., Li, F., Ramana, M.V., Praveen, P.S., Kim, D., Corrigan, C.E., Nguyen, H., Stone, E.A., Schauer, J.J., Carmichael, G.R., Adhikary, B., Yoon, S.C., 2007. Atmospheric brown clouds: Hemispherical and regional variations in long–range transport, absorption, and radiative forcing. *Journal of Geophysical Research–Atmospheres* 112, art. no. D22S21.

Ramanathan, V., Crutzen, P.J., Kiehl, J.T., Rosenfeld, D., 2001. Atmosphere–aerosols, climate, and the hydrological cycle. *Science* 294, 2119–2124.

Reddy B. S, Kumar, Y. B., 2013. Micro pulse lidar as a tool for active remote sensing of atmospheric particulate. *International Journal of Engineering and Technology* 5, 3394–3403.

Remer, L.A., Kaufman, Y.J., 2006. Aerosol direct radiative effect at the top of the atmosphere over cloud free ocean derived from four years of modis data. *Atmospheric Chemistry and Physics* 6, 237–253.

Ricchiazzi, P., Yang, S.R., Gautier, C., Sowle, D., 1998. SBDART: A research and teaching software tool for plane–parallel radiative transfer in the Earth's atmosphere. *Bulletin of the American Meteorological Society* 79, 2101–2114.

Salomonson, V.V., Barnes, W.L., Maymon, P.W., Montgomery, H.E., Ostrow, H., 1989. MODIS–advanced facility instrument for studies of the earth as a system. *IEEE Transactions on Geoscience and Remote Sensing* 27, 145–153.

Satheesh, S.K., Moorthy, K.K., 2005. Radiative effects of natural aerosols: A review. *Atmospheric Environment* 39, 2089–2110.

Satheesh S.K., Krishna Moorthy, K.,and Srinivasan, J.,2004. Introduction to Aerosols and Impacts on Climate: Basic Concepts, ISRO GBP Scientific report, ISRO–GBP SR 05 2004.

Satheesh, S.K., Moorthy, K.K., 1997. Aerosol characteristics over coastal regions of the Arabian Sea. *Tellus Series B–Chemical and Physical Meteorology* 49, 417–428.

Schwartz, S.E., Andreae, M.O., 1996. Uncertainty in climate change caused by aerosols. *Science* 272, 1121–1122.

Shaw, G. E., Reagan, J. A., Herman, B. M., 1973. Investigations of atmospheric extinction using direct solar radiation measurements made with a multiple wavelength radiometer. *Journal of Applied Meteorology*, 12, 374–380.

Tan, J.H., Duan, J.C., Chen, D.H., Wang, X.H., Guo, S.J., Bi, X.H., Sheng, G.Y., He, K.B., Fu, J.M., 2009. Chemical characteristics of haze during summer and winter in Guangzhou. *Atmospheric Research* 94, 238–245.

Tripathi, S.N., Tare, V., Chinnam, N., Srivastava, A.K., Dey, S., Agarwal, A., Kishore, S., Lal, R.B., Manar, M., Kanwade, V.P., Chauhan, S.S.S., Sharma, M., Reddy, R.R., Gopal, K.R., Narasimhulu, K., Reddy, L.S.S., Gupta, S., Lal, S., 2006. Measurements of atmospheric parameters during Indian Space Research Organization Geosphere Biosphere Programme Land Campaign II at a typical location in the Ganga basin: 1. Physical and optical properties. *Journal of Geophysical Research–Atmospheres* 111, art. no. D23209.

Watson, J.G., 2002. Visibility: Science and regulation. *Journal of the Air & Waste Management Association* 52, 628–713.

Weingartner, E., Saathoff, H., Schnaiter, M., Streit, N., Bitnar, B., Baltensperger, U., 2003. Absorption of light by soot particles: Determination of the absorption coefficient by means of aethalometers. *Journal of Aerosol Science* 34, 1445–1463.

Wolff, G.T., 1984. On the nature of nitrate in coarse continental aerosols. *Atmospheric Environment* 18, 977–981.

Yu, H., Kaufman, Y.J., Chin, M., Feingold, G., Remer, L.A., Anderson, T.L., Balkanski, Y., Bellouin, N., Boucher, O., Christopher, S., DeCola, P., Kahn, R., Koch, D., Loeb, N., Reddy, M.S., Schulz, M., Takemura, T., Zhou, M., 2006. A review of measurement–based assessments of the aerosol direct radiative effect and forcing. *Atmospheric Chemistry and Physics* 6, 613–666.

Zhang, Q.H., Zhang, J.P., Xue, H.W., 2010. The challenge of improving visibility in Beijing. *Atmospheric Chemistry and Physics* 10, 7821–7827.